Computer Aided Identification and Classification Model of Traditional Chinese Medicine Physiotherapy Jewelry Design

Shaosha Bian[1,*] and Zhigang Hu[2]

[1]Department of Jewelry, Shaanxi Institute of International Trade and Commerce, Xianyang, Shaanxi 712046, China, 20161016@csiic.edu.cn
[2]Department of Design and Arts, Shaanxi University of Science and Technology, Xi'an, Shaanxi 710021, China, huzhigang@sust.edu.cn

Corresponding author: Shaosha Bian, 20161016@csiic.edu.cn

Abstract. Compared with traditional jewelry, physiotherapy jewelry has both decorative and practical effects, and can also be regarded as a microelectronic product to decorate and beautify the image. Therefore, the development of intelligent jewelry cannot be separated from the fashion attributes of wearable devices and the long-term wearable attributes. In this paper, the application of DL(Deep learning) in the computer-aided design of Chinese medicine physiotherapy jewelry is discussed. A data acquisition system is established by computer-aided technology, and an ECG identification and classification model is established based on DL. The spatial structure characteristics of ECG signals are obtained by convolution-pooling method, and then the next full connection layer is carried out, and the output information obtained from all connection layers is used as the input and output of GRU module. The results show that the accuracy, recall and F1 of this method are 0.892, 0.849 and 0.745, respectively, and the best results are achieved. It is proved the design of traditional Chinese medicine physiotherapy jewelry.

Keywords: Deep Learning; Computer Aided; Jewelry Design; Chinese Medicine Physiotherapy.
DOI: https://doi.org/10.14733/cadaps.2023.S7.72-83

1 INTRODUCTION

Traditional Chinese medicine physiotherapy jewelry should belong to a type of smart wearable products, and one of its characteristics is that it has practical and aesthetic functions. Some smart wearable products can fully consider users' needs in function and human-computer interaction, but often ignore users' aesthetic needs, and Chinese medicine physiotherapy jewelry beads just make up for this vacancy. People have a long history of wearing jewelry, so different people have formed their own mature and stable aesthetic standards. However, the market positioning of smart wearable products is to highlight the practical function of microelectronic technology, while the

aesthetic function is weakened. The production and consumption of information has become a new direction of industrial development, and major economic countries in the world are actively promoting the development of smart cities and intelligent manufacturing [1]. People's lifestyle is irreversibly approaching informatization, and it can be predicted that intelligent technology will be widely involved in the traditional lifestyle in the future. In the future, the promotion and popularization of Internet of Things information technology will promote the design of new jewelry categories and new experiences, and at the same time, it will inevitably realize the expansion of the consumer market, and the jewelry industry will be on the road of intelligent upgrading [2].

Compared with traditional jewelry, physiotherapy jewelry has both decorative and practical effects, and it can also be regarded as a microelectronic product to decorate and beautify the image, such as electronic watch with navigation, ring with NFC and photo, bracelet with blood pressure detection, etc [3]. The birth of wearable intelligent products just makes jewelry more vivid and rich in emotional expression, personalization and artistic cultural implication. While achieving the goal of emotional communication, it also enables the public to fulfill their pursuit of modern science and technology, which will definitely bring impact to the traditional market with monotonous functional styles. Based on the market demand for wearable monitoring and the progress of related technologies, research institutes and companies in various countries are competing to carry out research and development of wearable monitoring system [4]. This paper systematically analyzes the feasibility of the perfect combination of smart wearable products and traditional jewelry. The appearance of wearable products is still consistent with that of traditional products, because people pay attention to aesthetics and care about others' perception of themselves [5].

Thase et al. [6] Computer assistance can provide advanced treatment solutions and software in the field of computer aided diagnosis and treatment for clinical hospitals. Provide professional auxiliary diagnosis solutions and software working platform for physical therapy. Provide professional surgical navigation scheme and surgical navigation equipment for clinical treatment. Wright et al. [7] has conducted more explicit research on the impact of clinician support, focused on the investigation of clinical practice implementation, cost-benefit analysis and the use of technological progress. Including more explicit research on the impact of clinician support, investigation focusing on the implementation of clinical practice, cost-benefit analysis and the use of technological progress. This paper reviews the research progress of computer - assisted cognitive behavior therapy (CCBT) in medical environment. Computer assisted surgical operation is to transfer the technical parameters of the surgical plan to the computer after the surgical plan is completed. Wright et al. [8] transforms the planning parameters of the image space to the computer operation program through the mapping algorithm, and finally the computer completes the designated auxiliary surgical operation according to the predetermined surgical plan. With the improvement of computer level and the introduction of infrared tracking and positioning technology and artificial intelligence technology, Wright et al. [9] believes that computer aided navigation system should become mature, become an intelligent surgical assistant system, and be widely used in clinical work. Wright et al. [10] believes that computer assistance can not only reduce the possibility of errors only based on visual inspection and experience. Moreover, the accuracy of artificial knee and hip joint replacement is increased. Compared with traditional surgery, the accuracy of prosthesis force line is greatly improved, which is more conducive to prolonging the life of patients after surgery.

2 RESEARCH METHOD

2.1 Intelligent Jewelry Design Concept

In jewelry, metal materials are most commonly used. Materials include precious metals and base metals. Precious metals mainly include gold and silver, while base metals mainly include copper, aluminum, steel and so on. Besides metals, the most commonly used traditional materials are precious stones. Jewelry can not only decorate our clothes, but also set off our temperament, and

to a certain extent, it can better reflect personal aesthetics and cognition. Necklaces wrapped around the neck, rings active at the fingertips, and earrings shining in both ears all appear like elves in streets, shops, exhibitions and even art galleries. However, more and more attention has been paid to the connotation conveyed by jewelry. Especially, young people's pursuit of individuality and cognition of design concepts are growing. Similarly, they pay more and more attention to artistic jewelry.

Generally speaking, the development trend of traditional Chinese medicine jewelry design is the development trend of function and aesthetics. If we look at it more finely, it involves the development trend of each element and whether they can be organically combined with each other, such as category subdivision, function combination, application of color and material, etc. The categories of physiotherapy jewelry include earrings, brooches, pendants, bracelets and rings, as shown in Figure 1, among which ring bracelets and pendants account for the vast majority.

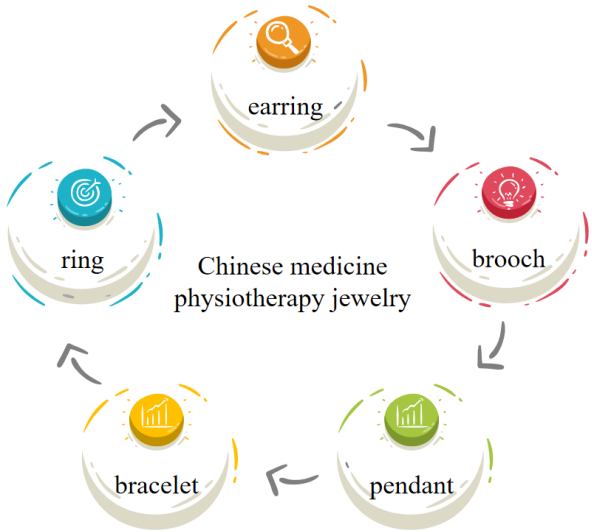

Figure 1: Categories of physiotherapy jewelry of traditional Chinese medicine.

Through the specific analysis of wearable devices, it can be seen that they mainly rely on core chip technology, intelligent application operating system technology and intelligent battery technology, and related auxiliary technologies include new material technology, intelligent communication technology and intelligent human-computer interaction application technology. Smart chips controlled by complex instructions are not competitive in smart chips because of their high energy consumption. At present, in the wearable era, the central processing unit is not the most critical factor, and the core position of intelligent sensors remains unshakable. At present, the characteristic design of intelligent jewelry is focused on user experience. Visual experience, interactive experience and specific functions have become important considerations that affect the user experience design of intelligent jewelry-related products.

2.2 Computer Aided Jewelry Design of Traditional Chinese Medicine Physiotherapy

When the static simulation of pulse signal analysis algorithm and motion noise reduction algorithm is carried out in the early stage, the actual collected pulse signal data is needed, and then the data acquisition system needs to be used. When the static algorithm simulation is completed and dynamic algorithm verification is needed, the algorithm verification system needs to be used. The system block diagram is shown in Figure 2.

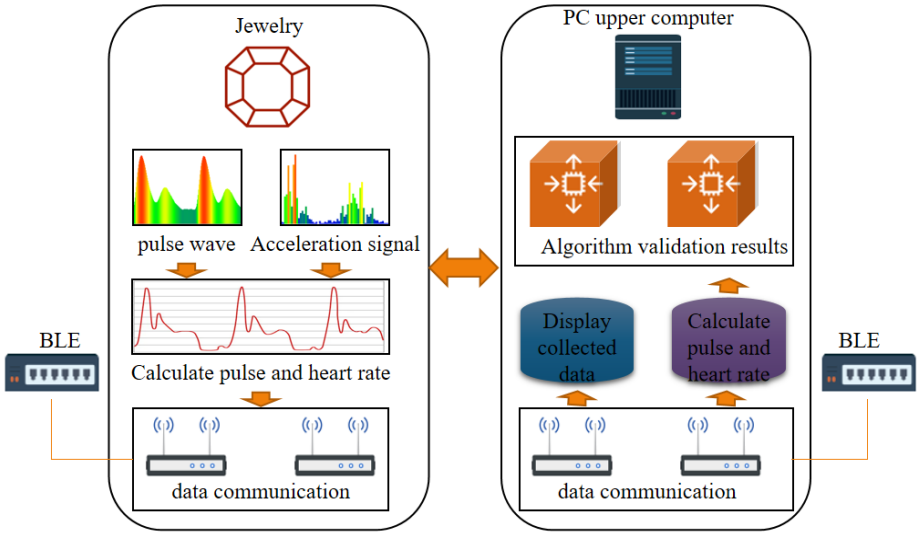

Figure 2: Block diagram of data acquisition system.

Firstly, the equivalent band-pass filter of Hal wavelet and its scale characteristics are analyzed. Then, according to the physical characteristics of pulse signal, the scale of wavelet decomposition is selected. The scaling function of Hal wavelet is a simple rectangular function, and its scaling function is represented by $\varphi(t)$ as follows:

$$\varphi(t)=\begin{cases}1, & 0<t<1\\ 0, & \text{others}\end{cases} \tag{1}$$

And the wavelet function of Hal wavelet is:

$$\psi(t)=\begin{cases}1, & 0<t<0.5\\ -1, & 0.5<t<1\\ 0, & \text{others}\end{cases} \tag{2}$$

In order to better reflect the overall change of acceleration in three axes, we define the standardized signal amplitude area SMA:

$$SMA=\frac{1}{t}\left(\int_0^t|a_x(t)|d_t+\int_0^t|a_y(t)|d_t+\int_0^t|a_z(t)|d_t\right) \tag{3}$$

Where $a_x(t), a_y(t), a_z(t)$ respectively represents the acceleration of human root point t on x, y, z axis.

We can regard all general actions of human body as the cross arrangement and combination of several basic actions.

$$S=\left[S_1,S_2,\cdots,S_n\right] \tag{4}$$

Based on the characteristic states, basic movements and their arrangement and combination, it can reflect the general action rules of human body and further analyze the behavior habits of human body. For example, the process from lying down to sitting up and then standing up includes two basic actions: sitting up and standing up, which can be judged by the method of complete matching. Extract the following basic actions and represent them in binary form:

Left-right alternating gait $S_1=00$, left-left alternating gait $S_2=01$, right left alternating gait $S_3=10$, right-right alternating gait $S_4=10$, bipedal to bipedal gait S_5.

We define the distance between two basic alternating actions:

$$d\left(S_x,S_y\right)=\frac{1}{2}\left[\left(S_{x1}\oplus S_{y1}\right)+\left(S_{x2}\oplus S_{y2}\right)\right] \tag{5}$$

That is, when the actions are consistent, the similarity distance is 0. Define the similarity distance between alternate action and double-legged action as 3.

2.3 Classification of ECG Recognition Based on DL

As an entity, intelligent devices meet the basic definition of traditional jewelry, such as being easy to carry, being able to decorate the human body, showing social status and wealth, and at the same time giving birth to the attribute of wearing experience. Such intelligent tools can be boldly called traditional Chinese medicine physiotherapy jewelry. For a long time, people regard watches and jewelry as the main wearable products. So, closely combining watches or jewelry with intelligent technology to provide people with intelligent services that traditional jewelry does not have will bring more humanized and high-quality interactive experience to customers. It can be mainly used to track and monitor women's sleep status, physiological status, etc., and can provide breathing training for women according to the final results. For traditional Chinese medicine physiotherapy jewelry products, not all the traditional jewelry making techniques are applicable, but the surface treatment techniques of metal or nonmetal, including mold pressing, polishing, electroplating, and inlay techniques, will still be widely used.

After a training sample is given, the significance of training an RBM lies in solving the parameter θ, such as the known joint probability distribution $P\left(v,h;\theta_{1,2}\right)$, so that the edge distribution $P\left(v;\theta_{1,2}\right)$ of neurons in the visible layer and the edge distribution $P\left(h;\theta_{1,2}\right)$ of neurons in the hidden layer can be obtained, as shown in Formula (6) and Formula (7) respectively.

$$P\left(v;\theta_{1,2}\right)=\sum_h P\left(v,h;\theta_{1,2}\right)=\frac{\sum_h e^{-E\left(v,h;\theta_{1,2}\right)}}{Z\left(\theta_{1,2}\right)} \tag{6}$$

$$P\left(h;\theta_{1,2}\right)=\sum_v P\left(v,h;\theta_{1,2}\right)=\frac{\sum_v e^{-E\left(v,h;\theta_{1,2}\right)}}{Z\left(\theta_{1,2}\right)} \tag{7}$$

According to the weighted sum vector Z of the input signal and the weight, the output result y is obtained after the activation function processing, and the expression is as follows:

$$y=f\left(Z\right)=f\left(\sum_{i=1}^{n}W_i\cdot x_i\right)=f\left(WX\right) \tag{8}$$

Operation of convolution layer: Let the input of m channel in the k-th layer be marked as c_m^k and the output as o_m^k, then the formula for calculation between input and output is:

$$o_m^k = f\left(c_m^k\right) \tag{9}$$

$$c_m^k = \sum_{i \in N_m} x_i^{k-1} * w_{ij}^k + b_m^k \tag{10}$$

Where f represents the excitation function, w_{ij}^k represents the convolution weight matrix, b_m^k represents the bias term, and N_m represents the features acquired by the $k-1$-th layer.

Pool layer calculation: if $pooling$ is used as the pool function, the output of the $k+1$ layer network is:

$$o_m^{k+1} = pooling\left(x_m^k\right) + b_m^{k+1} \tag{11}$$

The spatial structure characteristics of ECG signals are obtained by convolution-pooling method for many times, and then the next full connection layer is carried out, and the output information obtained from all connection layers is used as the input and output of GRU (gated recurrent unit) module. The CNN_GRU network model is shown in Figure 3.

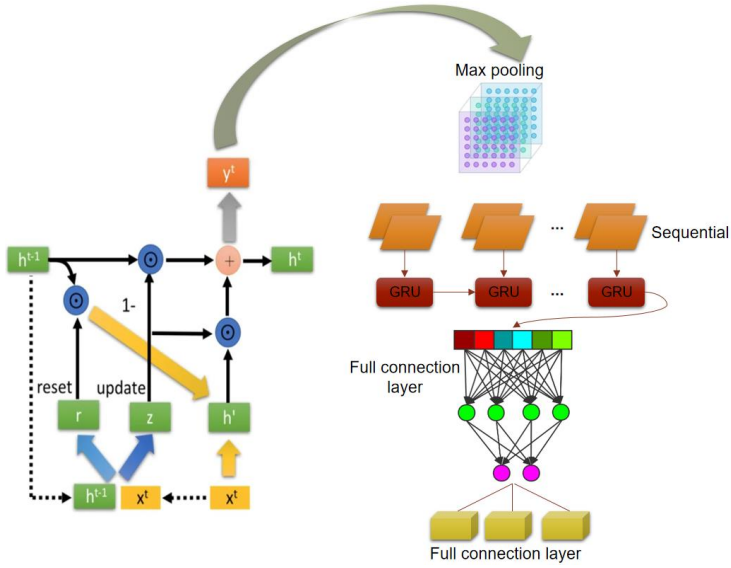

Figure 3: CNN_GRU network structure.

In order to make CNN model gradually converge to the global optimal value, the weights need to be initialized intelligently. In the convolution layer of CNN, these weights are represented as convolution kernels (or filters). The weights are randomly initialized according to the following uniform distribution:

$$W \sim U\left[-\frac{\sqrt{6}}{\sqrt{n_{in}+n_{out}}}, \frac{\sqrt{6}}{\sqrt{n_{in}+n_{out}}}\right] \tag{12}$$

Where n_{in}, n_{out} is the number of input and output neurons at the convolution kernel weight.

$$X^L = f\left(Z^L\right) = f\left(X * K^L + b^L\right) \tag{13}$$

$*$ represents convolution operation, Z^L represents the input value of the L st layer convolution, and X^L represents the feature mapping value obtained after the nonlinear activation function. f represents the activation function.

The training process of CNN in this study is essentially a supervised learning process. All the input data correspond to a real label, and the output value of the network is the predicted value of the input data. The training process of network is based on the back propagation of loss function, so as to optimize the network parameters and continuously reduce the loss.

$$L = \sum_{i=1}^{N} L\left(W, \left(y, x_1, x_2\right)^i\right) \tag{14}$$

$\left(y, x_1, x_2\right)^i$ is the i th sample pair, x_1, x_2 is the ECG sample in the sample pair, and y is the label of the sample pair.

Let $L^{(t)}$ be the negative logarithmic likelihood of y after a given $x^{(1)}, x^{(2)}, \cdots, x^{(t)}$, then the loss function:

$$\begin{aligned} &L\left(\left\{x^{(1)}, x^{(2)}, \cdots, x^{(t)}\right\}, \left\{y^{(1)}, y^{(2)}, \cdots, y^{(t)}\right\}\right) = \sum_t L^{(t)} = \\ &-\sum_t \log p_{\mathrm{mod}el}\left(y^{(t)} \middle| \left\{x^{(1)}, x^{(2)}, \cdots, x^{(t)}\right\}\right) \end{aligned} \tag{15}$$

Where $p_{\mathrm{mod}el}\left(y^{(t)} \middle| \left\{x^{(1)}, x^{(2)}, \cdots, x^{(t)}\right\}\right)$ needs to read the item corresponding to $y^{(t)}$ in the model output vector $\hat{y}^{(t)}$.

$$\nabla_{h(t)} L = \left(\frac{\partial h^{(t+1)}}{\partial h^{(t)}}\right)\left(\nabla_{h(t+1)} L\right) + \left(\frac{\partial o^{(t)}}{\partial h^{(t)}}\right)^T \left(\nabla_{o(t)} L\right) = W^T\left(\nabla_{h(t+1)} L\right) diag\left(\left(1-h^{(t+1)}\right)^2\right) + V^T\left(\nabla_{o(t)} L\right) \tag{16}$$

Wherein, represents the diagonal matrix of $diag\left(\left(1-h^{(t+1)}\right)^2\right)$ containing element $\left(1-h^{(t+1)}\right)^2$ Is the hyperbolic tangent Jacobian matrix associated with the hidden layer element i at time $t+1$.

3 RESULT ANALYSIS AND DISCUSSION

The experimental data source of this paper is MIT-BIH arrhythmia database. According to the standard of AAMI, the final purpose of this paper is to classify the beat samples in the database into four types of arrhythmia beats: normal heartbeat (N), supraventricular ectopic heartbeat (S), ventricular ectopic heartbeat (V), and fusion heartbeat (F). Division in 1000 sampling points for a sample data, is also constructs the 3600 samples, each type of signal of 600 samples respectively. That is, the generalization ability of the proposed model is fully verified by using the transformation domain dataset. The experimental environment is: Microsoft Windows 10 operating system; The GPU model is NVIDIA Telsa P100, and the operating memory is 16GB; Using Python programming language, the DL framework is Tensorflow.

Experimental parameter setting: epochs is set to 10; batch_ Size is set to 64; Number learning_ The rate is set to 0.001; Adam is selected as the optimizer; Dropout represents that neurons are randomly discarded during the training process, and the parameter rate is set to 0.1; The loss function uses cross entropy loss.

This paper builds a CNN model with different network layers. After several groups of comparison experiments, this paper finally sets the number of hidden layers of CNN model as 3, which results in the best classification effect. See Table 1 for example.

Hidden layers	*Overall accuracy/%*
1	95.887
2	91.758
3	96.008
4	92.451
5	93.85
6	94.66
7	94.769

Table 1: Comparison between different hiding layers and accuracy.

The ECG classification method based on integrated one-dimensional CNN is verified with the data set after data balance processing; And set up a control experiment. Before integrating the results of the base learner, the training accuracy rate and loss rate are shown in Figure 4 and Figure 5:

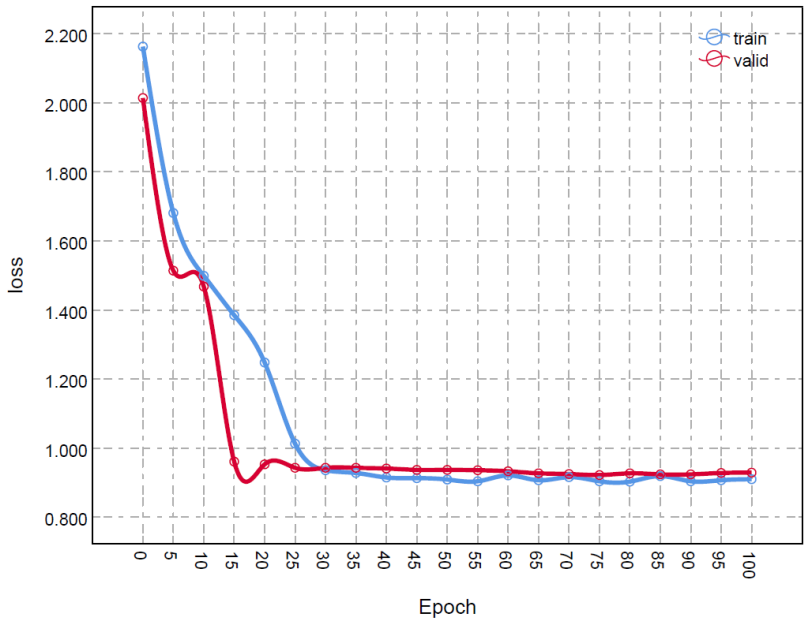

Figure 4: CNN_ Training accuracy rate of GRU.

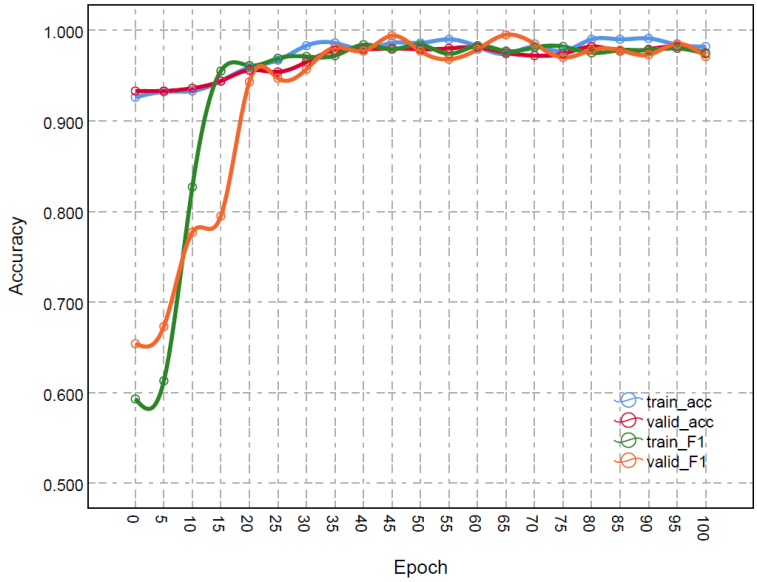

Figure 5: CNN_ Training loss rate of GRU.

The curve of loss rate change shows that the loss value drops significantly at the beginning of the training.

In order to evaluate the performance of the proposed in this paper more reasonably, the confusion matrix of this classification task is presented to verify the classification effect of the ECG 4. The confusion matrix of the final classification results is shown in Table 2 and Figure 6.

Category	*N*	*S*	*V*	*F*
N	8680	9	87	152
S	536	7601	8922	7104
V	3433	2690	7229	4335
F	356	636	5361	6853

Table 2: ECG classification confusion matrix.

Different cross validation was used in the study. Index the training set according to the experimental results and the results are shown in Table 3 and Figure 7.

Experiment achieves the best results in terms of accuracy, recall rate and F1, which are respectively 0.892, 0.849 and 0.745. This is because the CNN_GRU model combines temporal and spatial feature information to fully examine the local and global features of the model, and integrates the global features with the local features. The identity mapping is realized by using residual block. The correct recognition rate, stability and generalization ability of the network are obviously improved, and the misjudgment rate is reduced. This model has good performance in pattern recognition of similar data samples and can be used for classification and recognition of large sample data sets such as time-varying signals.

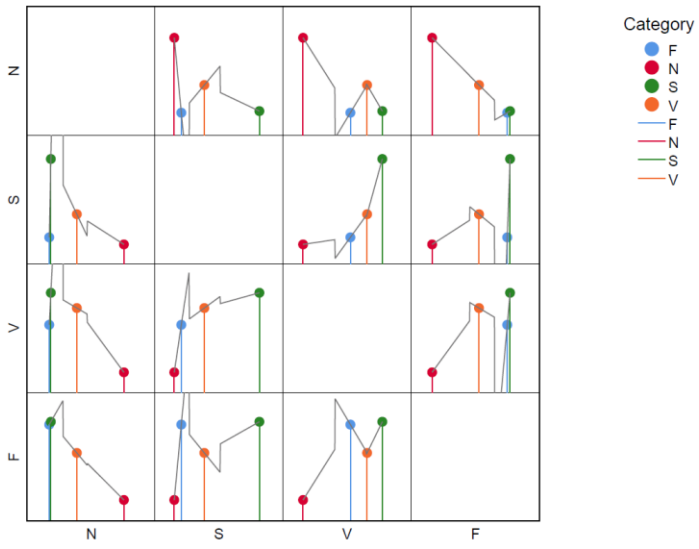

Figure 6: ECG classification confusion matrix.

Model	*Accuracy*	*Recall*	*F1*
CNN	0.75	0.792	0.706
RBM	0.68	0.791	0.719
LSTM	0.804	0.712	0.701
ResNet	0.768	0.744	0.7
Depth residual CNN	0.808	0.739	0.721
our	0.892	0.849	0.745

Table 3: Comparison experiment.

4 CONCLUSION

Today, the current society is a society in which mobile Internet technology is gradually becoming mature, and also an era in which digital information and industrialization are growing. Compared with the existing smart bracelets, the traditional Chinese medicine physiotherapy jewelry not only has a fashionable and compact appearance, but also can perfectly display the aesthetic personality of the wearer. In this paper, the application of DL in computer aided jewelry design of traditional Chinese medicine therapy is discussed. A data acquisition system is established with computer aided technology, and an ECG recognition and classification model is established based on DL. The research results show that the accuracy rate, recall rate and F1 are 0.892, 0.849 and 0.745 respectively, and the method in this paper has achieved the best results. This model has good performance in pattern recognition of similar data samples and can be used for classification and recognition of large sample data sets such as time-varying signals.

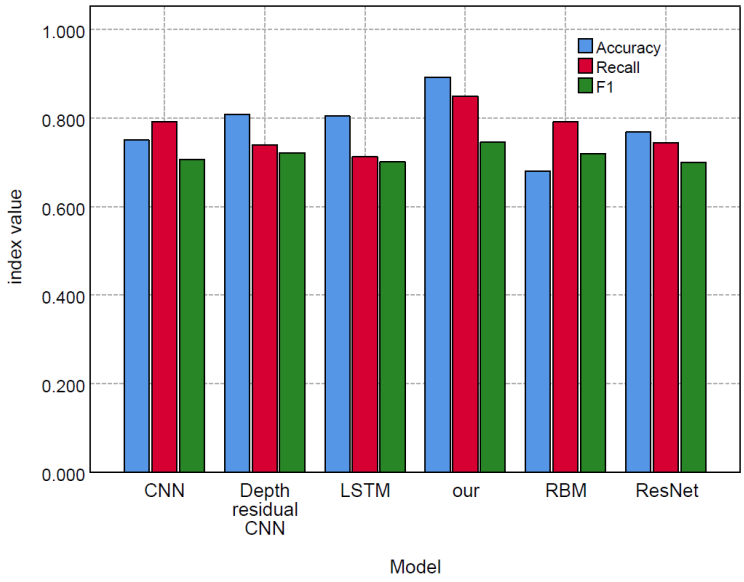

Figure 7: Statistical comparison of experimental results.

5 ACKNOWLEDGEMENTS

This work was supported by 2022 general special scientific research plan of Shaanxi Provincial Department of Education: Research on the Application of Traditional Chinese Medicine with Odour Physiotherapy Value in the Design of Functional Jewelry (No. 22JK0024); School level scientific research project of Shaanxi Institute of International Trade and Commerce in 2021: Research on the Application of Mineral Drugs with Physiotherapy Value in the Design of Functional Jewelry (No. SMZX202146).

Shaosha Bian, https://orcid.org/0000-0002-2830-364X
Zhigang Hu, https://orcid.org/0000-0002-8703-4259

REFERENCES

[1] Fuchs, H.; Elia, A.; Resch, A.-F.; Kuess, P.; Lühr, A.; Vidal, M.; Georg, D.: Computer - assisted beam modeling for particle therapy, Medical Physics, 48(2), 2021, 841-851. https://doi.org/10.1002/mp.14647

[2] Heesacker, M.; Perez, C.; Quinn, M.-S.; Benton, S.: Computer - assisted psychological assessment and psychotherapy for collegians, Journal of Clinical Psychology, 76(6), 2020, 952-972. https://doi.org/10.1002/jclp.22854

[3] Li, K.; Vakharia, V.-N.; Sparks, R.; França, L.-G.; Granados, A.; McEvoy, A.-W.; Duncan, J.-S.: Optimizing trajectories for cranial laser interstitial thermal therapy using computer-assisted planning: a machine learning approach, Neurotherapeutics, 16(1), 2019, 182-191. https://doi.org/10.1007/s13311-018-00693-1

[4] Morimoto, T.; Matsuda, Y.; Matsuoka, K.; Yasuno, F.; Ikebuchi, E.; Kameda, H.; Kishimoto, T.: Computer-assisted cognitive remediation therapy increases hippocampal volume in patients with schizophrenia: a randomized controlled trial, BMC psychiatry, 18(1), 2018, 1-8. https://doi.org/10.1186/s12888-018-1667-1

[5] Thase, M.-E.; McCrone, P.; Barrett, M.-S.; Eells, T.-D.; Wisniewski, S.-R.; Balasubramani, G.-K.; Wright, J.-H.: Improving cost-effectiveness and access to cognitive behavior therapy for depression: providing remote-ready, computer-assisted psychotherapy in times of crisis and beyond, Psychotherapy and psychosomatics, 89(5), 2020, 307-313. https://doi.org/10.1159/000508143

[6] Thase, M.-E.; Wright, J.-H.; Eells, T.-D.; Barrett, M.-S.; Wisniewski, S.-R.; Balasubramani, G.-K.; Brown, G.-K.: Improving the efficiency of psychotherapy for depression: computer-assisted versus standard CBT, American Journal of Psychiatry, 175(3), 2018, 242-250. https://doi.org/10.1176/appi.ajp.2017.17010089

[7] Wright, J.-H.; McCray, L.-W.; Eells, T.-D.; Gopalraj, R.; Bishop, L.-B.: Computer-assisted cognitive-behavior therapy in medical care settings, Current psychiatry reports, 20(10), 2018, 1-9. https://doi.org/10.1007/s11920-018-0947-2

[8] Wright, J.-H.; Mishkind, M.; Eells, T.-D.; Chan, S.-R.: Computer-assisted cognitive-behavior therapy and mobile apps for depression and anxiety, Current psychiatry reports, 21(7), 2019, 1-9. https://doi.org/10.1007/s11920-019-1031-2

[9] Wright, J.-H.; Mishkind, M.: Computer-assisted CBT and mobile apps for depression: assessment and integration into clinical care, Focus, 18(2), 2020, 162-168. https://doi.org/10.1176/appi.focus.20190044

[10] Wright, J.-H.; Owen, J.-J.; Richards, D.; Eells, T.-D.; Richardson, T.; Brown, G.-K.; Thase, M.-E.: Computer-assisted cognitive-behavior therapy for depression: a systematic review and meta-analysis, The Journal of clinical psychiatry, 80(2), 2019, 3573. https://doi.org/10.4088/JCP.18r12188